THE JOURNAL OF PHYSICAL CHEMISTRY A

Article

pubs.acs.org/JPCA

Ultrafast Long-Distance Excitation Energy Transport in Donor–Bridge–Acceptor Systems

Guillaume Duvanel, Jakob Grilj, and Eric Vauthey*

Department of Physical Chemistry, University of Geneva, 30 Quai Ernest-Ansermet, CH-1211 Geneva 4, Switzerland

Supporting Information

ABSTRACT: The excited-state dynamics of two energy donor–bridge–acceptor (D–B–A) systems consisting of a zinc tetraphenylporphyrin (ZnP) and a free base tetraphenylporphyrin (FbP) bridged by oligo-*p*-phenyleneethynylene units with different substituents has been investigated using ultrafast spectroscopy. These systems differ by the location of the lowest singlet excited state of the bridge, just above or below the S_2 porphyrin states. In the first case, Soret band excitation of the porphyrins is followed by internal conversion to the local S_1 state of both molecules and by a S_1 energy transfer from the ZnP to the FbP end on the 10 ns time scale, as expected for a center-to-center distance of about 4.7 nm. On the other hand, if the bridge is excited, the energy is efficiently transferred within 1 ps to both porphyrin ends. Selective bridge excitation is not possible with the second system, because of the overlap of the absorption bands. However, the time-resolved spectroscopic data suggest a reversible conversion between the D*(S_2)–B–A and D–B*(S_1)–A states as well as a transition from the D–B*(S_1)–A to the D–B–A* states on the picosecond time scale. This implies that the local S_2 energy of the ZnP end can be transported stepwise to the FbP end, i.e., over about 4.7 nm, within 1 ps with an efficiency of more than 0.2.

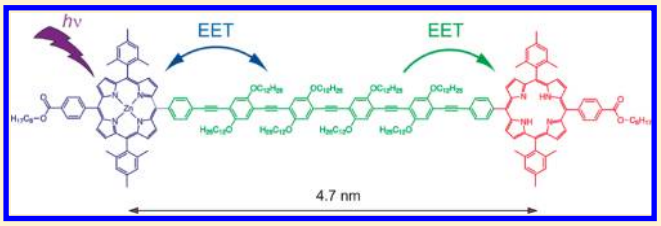

INTRODUCTION

Over the past years, substantial effort has been invested in the synthesis and investigation of multichromophoric molecules designed for undergoing efficient intramolecular charge or excitation energy transfer (EET) and thus mimicking the light-harvesting complexes and/or the reaction center of natural photosynthetic organisms.[1−18] Many of these systems consist of porphyrins covalently bound to a bridging unit. The primary role of the bridge is to replace the protein scaffold of the natural systems, and to act as a spacer for controlling the coupling between the chromophoric units through the distance and/or the relative orientation. However, it was quickly realized that, in most cases, the bridge is not operating as an inert building block, but favors charge and excitation energy transfer between the units via through-bond interactions.[6,19−29] Consequently, it is now well established that the distance dependence of these tunneling processes, i.e., electron transfer and EET via the Dexter mechanism, is not an intrinsic property of the bridge, but is influenced by the energy gap between the electronic levels of the bridge and of the electron/energy donor.[26,29] Indeed, at constant donor–acceptor distance, the transfer rate constant was found to increase upon lowering the donor–bridge energy gap, until the process became sequential, i.e., until the charge or the excitation energy localized on the bridge before being further transferred to the acceptor unit. In such a case, the transfer mechanism changes from coherent tunneling through the bridge to incoherent hopping via the bridge.[30−32] Independently of the mechanism, long-distance, ultrafast, and irreversible charge/excitation energy transfer is a common goal for many applications, including artificial photosynthesis and molecular electronics.

We present here the results of our efforts toward long-distance, ultrafast, and irreversible EET in two donor–bridge–acceptor (D–B–A) systems (Chart 1). They consist of a zinc tetraphenylporphyrin (ZnP) unit and a free base tetraphenylporphyrin unit (FbP) bridged by a long oligomeric *p*-phenyleneethynylene (OPE) unit, yielding a center-to-center distance of about 4.7 nm. The difference between these two systems resides in the presence or not of alkoxy substituents on the bridge. Previous investigations of the photophysics of the two bridging molecules (B_1 and B_2) have shown that their S_1 energies amount to 3.23 and 2.84 eV, respectively, i.e., just above and below that of ∼2.9 eV associated with the Soret band of the porphyrins.[33] Furthermore, because of the relatively long-lived S_2 state of ZnP, between 1.5 and 2.4 ps depending on the solvent,[34−36] and of the strong $S_2 \leftarrow S_0$ transition dipole moment, S_2 excitation energy hopping has been shown to be operative in ZnP arrays.[7,37]

Here we investigate, using ultrafast spectroscopy, whether Soret band excitation of the ZnP unit in these D–B–A systems could be followed by S_2 EET to the bridge. As illustrated by the energy level scheme in Figure 1, this transfer should be followed by a further EET from the bridge toward either the ZnP or FbP unit. As the porphyrins are far apart, and as their local S_1 states are much lower than that of the bridge, both of

Received: November 22, 2012
Revised: January 11, 2013
Published: January 17, 2013

Chart 1. Chemical Structures of the D−B−A Systems and of D−B_2

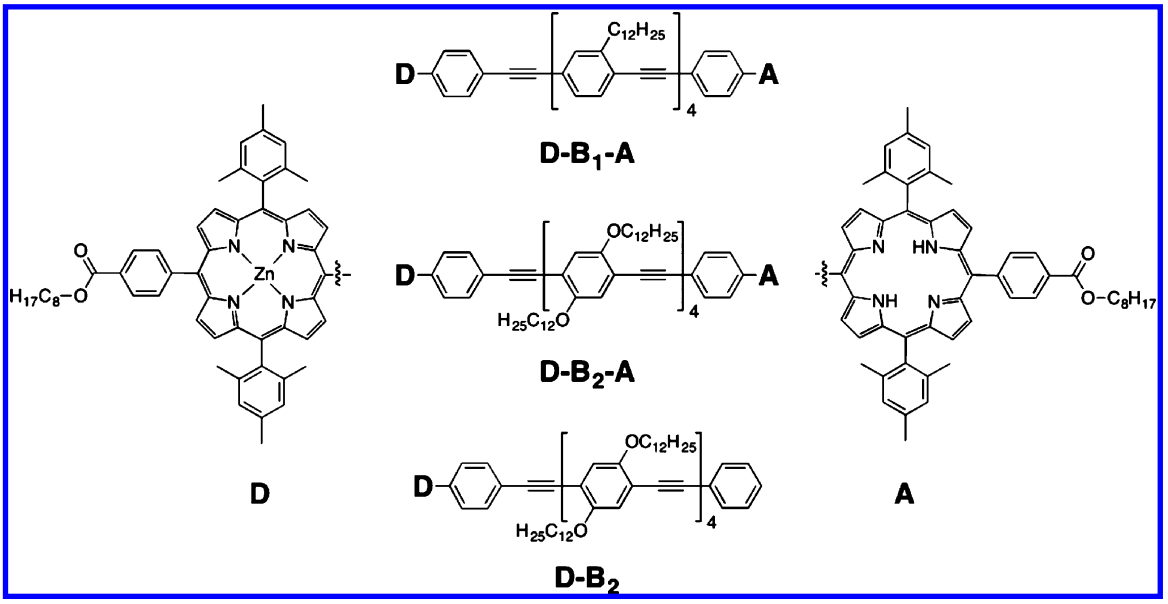

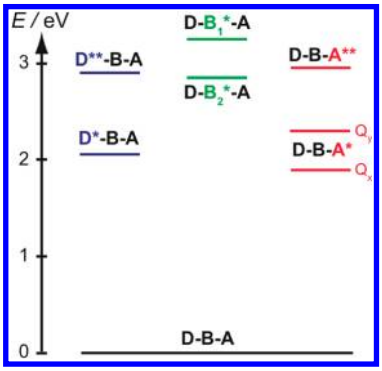

Figure 1. Energy level scheme of the two D−B−A systems based on the absorption and emission spectra of the individual constituents. The double asterisk corresponds to a local S_2 excited state.

them can be expected to act as energy traps. If the excitation energy is eventually trapped on the FbP moiety, the whole process corresponds to an ultrafast long-distance EET. In order to better understand the influence of the bridge on the excited-state properties of ZnP, the photophysics of D−B_2 was also investigated.

EXPERIMENTAL SECTION

Samples. The D−B_1−A, D−B_2−A, and D−B_2 systems were given by Prof. A. Gossauer (Chemistry Department of the University of Fribourg) and were used as received. All measurements were performed in toluene, which was of analytical grade (Acros Organics, p.a.) and was used without further purification.

Steady-State Spectroscopy. Absorption spectra were recorded on a Cary 50 spectrophotometer, whereas stationary fluorescence was measured on a Cary Eclipse fluorimeter. All fluorescence spectra were corrected for the wavelength-dependent sensitivity of the detection.

Time-Resolved Fluorescence. Fluorescence dynamics on the nanosecond time scale was measured using the same time-correlated single photon counting (TCSPC) setup as described in refs 38 and 39. Excitation was carried out with ∼60 ps pulses generated by a laser diode at 395 nm (PicoQuant Model LDH-PC-400B), and fluorescence was detected at the magic angle. The full width at half-maximum (fwhm) of the instrument response function (IRF) was around 200 ps. Faster fluorescence dynamics was measured using fluorescence up-conversion (FU), as described previously.[40,41] Excitation was performed between 380 and 420 nm using the frequency-doubled output of a Kerr lens mode-locked Ti:sapphire laser (Tsunami, Spectra-Physics). The polarization of the pump pulses was at the magic angle relative to that of the gate pulses. The pump intensity on the sample was on the order of 5 $\mu J \cdot cm^{-2}$, and the fwhm of the instrument response function was ca. 210 fs. The sample solutions were located in a 0.4 mm thick rotating cell and had an absorbance of about 0.1 at the excitation wavelength.

Transient Absorption (TA). The TA setup has been described in detail earlier.[42,43] Excitation was performed at 400 nm with the frequency-doubled output of a standard 1 kHz amplified Ti:sapphire system (Spectra-Physics). The pump intensity on the sample was ca. 1−2 $mJ \cdot cm^{-2}$. The polarization of the probe pulses was at the magic angle relative to that of the pump pulses. All spectra were corrected for the chirp of the white-light probe pulses. The fwhm of the response function was ca. 150 fs. The sample solutions were placed in a 1 mm thick quartz cell and were continuously stirred by N_2 bubbling. Their absorbance at the excitation wavelength was around 0.3.

Quantum Chemical Calculations. Ground-state gas-phase geometry optimization was performed at the density functional level of theory (DFT) using the B3LYP functional[44] and a [3s2p1d] basis set.[45] Electronic vertical excitation energies were computed with time-dependent density functional theory (TD-DFT) using the same functional and basis set.[46] The calculations were carried out using Turbomole version 6.1.[47]

RESULTS

Steady-State Spectroscopy. The absorption spectra of D−B_1−A and D−B_2−A in toluene are illustrated in Figure 2. These spectra show the typical Q and Soret bands of the porphyrins.[48] The Q-band spectral region (500−670 nm) of both systems is the composite of the absorption spectra of ZnP

dx.doi.org/10.1021/jp311540x | J. Phys. Chem. A 2013, 117, 918−928

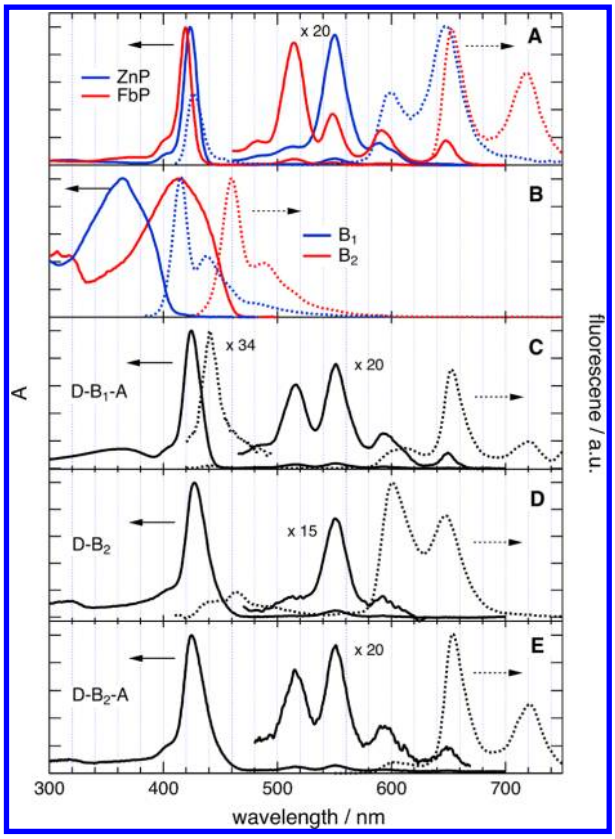

Figure 2. Absorption (continuous) and emission (dotted) spectra of (A) ZnP and FbP, (B) B_1 and B_2, (C) D−B_1−A (375 nm excitation), (D) D−B_2 (400 nm excitation), and (E) D−B_2−A (400 nm excitation) in toluene. Note that the fluorescence spectra of the D−B−A's depend on the excitation wavelength.

and FbP. This is not the case for the Soret band region, where the Soret bands of D−B_1−A and D−B_2−A are broader by about 10 and 30%, respectively, than that of the composite of the ZnP and FbP spectra normalized according to the absorption coefficient. Moreover, the Soret bands of both D−B−A's are ∼220 cm^{-1} red shifted relative to the composite spectra. The broad absorption band at 364 nm in the D−B_1−A spectrum is due to the OPE bridge B_1. The position of this band in D−B_1−A is essentially the same as that measured with B_1 in toluene.[33] On the other hand, the first absorption band of the B_2 bridge in toluene is centered at 414 nm and overlaps the Soret band of the porphyrins.[33] The absorption of B_2 is probably responsible for the stronger broadening of the Soret band of D−B_2−A compared to D−B_1−A. This is supported by the Soret band of D−B_2 that exhibits the same ∼30% broadening. The broadening and shift of the Soret band of the D−B−A's point to substantial perturbation of the porphyrin electronic structure by the bridge. Indeed, the presence of the bridge leads to a lowering of the symmetry of the porphyrins that, in the case of ZnP, should result in a suppression of the degeneracy of the B and Q states. However, this perturbation is not strong enough to split the absorption bands.

From these spectra, one can conclude that the lowest electronic state of both D−B−A's is centered on the FbP unit, whereas the next one is localized on the ZnP. To simplify the discussion, these states will be further on named local S_1 FbP and local S_1 ZnP states.

For both D−B−A's, TD-DFT calculations point to the presence of more than 20 electronic excited states below 3 eV. For D−B_1−A, the lowest and second lowest excited states are predicted to be mostly localized on the FbP and ZnP units, respectively, in good agreement with observation (Figure S1, Supporting Information). On the other hand, the calculations with D−B_2 and D−B_2−A predict that the first excitation corresponds to a one-electron transition from the HOMO (highest occupied molecular orbital), localized mostly on B_2, to the LUMO (lowest unoccupied molecular orbital), centered on ZnP for D−B_2 or on FbP for D−B_2−A (Figure S2, Supporting Information). Thus, the lowest excited state should have a strong charge transfer character, in clear disagreement with the experimental spectra that show that the first transitions are localized on the porphyrins. This discrepancy originates from the difficulty of reliably reproducing the first transition energies of B_1 and B_2, with the calculated energies being 2.7 and 2.4 eV, respectively, whereas the measured ones are approximately 0.6 eV higher. This important underestimation seems to be mostly due to the planarity of the bridges in the optimized geometries that favors conjugation.[49] It has been shown that the barrier for torsion of the phenyl groups around the single bonds of OPEs in the ground state is small and that these molecules are consequently not planar at room temperature.[50,51] As a consequence, conjugation is smaller and the transition energy is larger than predicted for planar OPEs. Another contribution to this discrepancy is the well-known tendency of TD-DFT to underestimate the energy of charge transfer excited states when using standard functionals like the B3LYP.[52] Because of these problems, the calculated energy ordering of the molecular orbitals (MOs) of the D−B−A's is not reliable. However, these calculations are still useful to appreciate the mixing of the bridge and porphyrin MOs. In particular, they reveal that, when the bridge and the porphyrins have MOs of similar energies, the corresponding D−B−A MOs are delocalized over both bridge and porphyrins (Figure S2, Supporting Information). This is no longer the case when the bridge and porphyrin MOs have dissimilar energies. In these cases, the D−B−A MOs are localized on either the bridge or a porphyrin (Figure S1, Supporting Information). D−B_2−A, for which the bridge excited state is almost isoenergetic with the local S_2 states of the porphyrins, corresponds most probably to the first case, i.e., delocalized MOs. On the other hand, D−B_1−A should be closer to the second case (localized MOs), because the bridge excited state is substantially higher than the local S_2 porphyrin states.

The fluorescence spectra of the D−B−A's are dominated by three bands at 600, 650, and 720 nm (Figure 2). These spectra resemble closely the composites of the emission spectra of ZnP and FbP. The first and last bands can be ascribed to ZnP and FbP, respectively, whereas that at 650 nm is due to both. The relative intensity of these bands depends substantially on the excitation wavelength. Up to 500 nm, the fluorescence excitation spectra measured at 600 and 720 nm exhibit mainly the Q bands of ZnP and FbP, respectively (Figure S3, Supporting Information). In the Soret band region, the excitation spectra at 600 nm are slightly red shifted relative to those at 720 nm, in agreement with the relative positions of the Soret bands of ZnP and FbP. In D−B_1−A, both excitation spectra additionally exhibit the bridge band around 365 nm (Figure S3, Supporting Information).

From these spectra, one can conclude that, if occurring, the transfer of the local S_1 excitation from the ZnP to the FbP unit

dx.doi.org/10.1021/jp311540x | J. Phys. Chem. A 2013, 117, 918−928

is not very efficient. If it were, the emission spectra of the D−B−A's would be independent of the excitation wavelength in the Q-band region and should only exhibit the FbP bands. On the other hand, the Soret bands of the porphyrins overlap so much that it is not possible to determine whether local S_2 excitation of the ZnP end results in emission of the FbP end.

Upon excitation below 430 nm, additional emission bands at 440 and 460 nm can be observed with D−B_1−A and D−B_2, respectively (Figure 2C,D). With D−B_2−A, only a small feature close to the limit of detection can be observed (Figure 2E). These bands can be ascribed to the local S_2 fluorescence of ZnP and to the local emission of the bridges.[33,53] Indeed, the fluorescence excitation spectrum of D−B_1−A at 440 nm exhibits both the Soret band and the bridge band, whereas the excitation spectrum of D−B_2 at 460 nm matches very well the broadened Soret band. The S_2 fluorescence of ZnP culminates at 427 nm with a red edge extending to ∼470 nm (Figure 2A). However, its very small Stokes shift favors reabsorption, and therefore, the measured emission spectrum is usually red shifted unless very dilute ZnP solutions are used.[53] The broadening of the Soret band of the D−B−A's most certainly causes a substantial reabsorption of the blue part of ZnP S_2 fluorescence. On the other hand, the fluorescence spectrum of B_1 consists of a sharp band at 415 nm with a pronounced vibronic band at 440 nm (Figure 2B).[33] In this case again, the absence of the 415 nm feature in the emission spectrum of D−B_1−A can be accounted for by reabsorption. The fluorescence spectrum of B_2 has a shape very similar to that of B_1 but culminates at 460 nm with the vibronic band at 490 nm.[33] The band measured with D−B_2 resembles very much that of B_2 but is broadened on the blue side, most probably because of the local S_2 emission of the ZnP. Figures S4 and S5 (see the Supporting Information) further support that the fluorescence of D−B_1−A and D−B_2 around 450 nm is well accounted for by a contribution from both ZnP and the bridge.

In D−B_2 and D−B_2−A, neither the porphyrins nor the bridge can be selectively excited due to the strong overlap of their absorption bands. By contrast, with D−B_1−A, almost exclusive bridge excitation can be carried out at 365 nm. By scaling the relative intensity of the fluorescence spectra of the three constituents according to their fluorescence quantum yields (i.e., Φ_f(ZnP):Φ_f(B_1):Φ_f(FbP) = 0.033:0.91:0.11),[33,54,55] it appears that their relative contribution to the emission spectrum of D−B_1−A upon 365 nm excitation is ZnP:B_1:FbP = 2:∼0.01:1 (Figure S5, Supporting Information). This unambiguously shows that EET occurs from the bridge to the ZnP and FbP ends. Assuming negligible absorbance of the porphyrins at 365 nm, the efficiencies of these EETs to ZnP and FbP are about 0.66 and 0.33, respectively.

Time-Resolved Fluorescence. The fluorescence dynamics was first investigated on the nanosecond time scale using TCSPC with 395 nm excitation. At this wavelength, both porphyrins are excited, with FbP having an absorption coefficient by a factor of about 2.5 larger than that of ZnP. Additionally both B_1 and B_2 absorb substantially as well.

The fluorescence of both D−B−A's at 710 nm decays exponentially with a time constant of about 11 ns (Table 1), whereas, at shorter wavelength, it exhibits a biexponential decay with the same ∼11 ns time constant and with an additional time constant around 2 ns (Table 1, Figure S6 in the Supporting Information). The relative amplitude of this faster component increases with decreasing wavelength and becomes dominant (≥95%) around 600 nm. These two lifetimes agree

Table 1. Time Constants, τ_f, and Relative Amplitudes (in Parentheses) Obtained from Analysis of the Fluorescence Time Profiles Measured at Different Emission and Excitation Wavelengths, λ_f and λ_e[a]

		τ_f		
λ_e/nm	λ_f/nm	D−B_1−A	D−B_2	D−B_2−A
395	710	10.7 ns		1.5−2 ns (−0.15)
				10.8 ns
395	590	2.04 ns	2.24 ns	1.72 ns
380	460	380 fs (0.8)		
		4 ps (0.2)		
380	650	800 fs (−0.4)		
		>1 ns		
420	440	820 fs		
420	650	800 fs (−0.5)		
		>1 ns		
400	430[b]		350 fs (0.53)	130 fs (0.56)
			1.1 ps (0.42)	480 fs (0.44)
			850 ps (0.05)[c]	
400	520[b]		350 fs (0.47)	130 fs (0.73)
			1.1 ps (0.39)	480 fs (0.26)
			850 ps (0.14)[c]	850 ps (0.01)[c]

[a]The errors on the time constants are around ±5% and ±10% for TCSPC and FU measurements, respectively. [b]The fluorescence profiles at these two wavelengths were analyzed globally. [c]Ascribed to free B_2 impurities.

well with those reported for the individual porphyrins, namely around 2 and 11 ns for ZnP and FbP, respectively.[4,54] This clearly confirms that the lowest electronic excited states of the D−B−A's are localized on the porphyrin ends.

On the other hand, the fluorescence decay of D−B_2 is exponential throughout the whole 590−690 nm band with a time constant of 2.24 ns. As shown in Table 1 and Figure 3, this

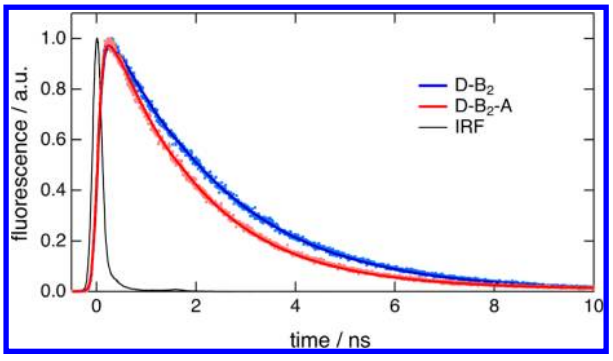

Figure 3. Fluorescence time profiles measured by TCSPC with D−B_2 and D−B_2−A at 590 nm upon 395 nm excitation.

is significantly longer that of 1.72 ns measured with D−B_2−A. This difference can be ascribed to the occurrence of EET between the ZnP end and the FbP end in D−B_2−A. Because the ZnP unit cannot be selectively excited, about 85% of the rise of the FbP fluorescence at 700 nm is prompt, and only a small rising component with an ∼1.5−2 ns time constant that corresponds to the excitation of FbP via EET can be observed. An EET rate constant of $(7.4\ \text{ns})^{-1}$ can be deduced from the difference of fluorescence lifetimes between D−B_2 and D−B_2−A. Such an EET might also take place in D−B_1−A. However, as the D−B_1 analogue was not available for comparison,

dx.doi.org/10.1021/jp311540x | J. Phys. Chem. A 2013, 117, 918−928

occurrence of this process could not be evidenced by fluorescence.

The fluorescence dynamics in the 430−500 nm region due to the local S_2 ZnP and S_1 bridge states was much too fast to be resolved by TCSPC and was measured by FU. As depicted in Figure 4A, the fluorescence time profile of D−B_1−A at 440 nm

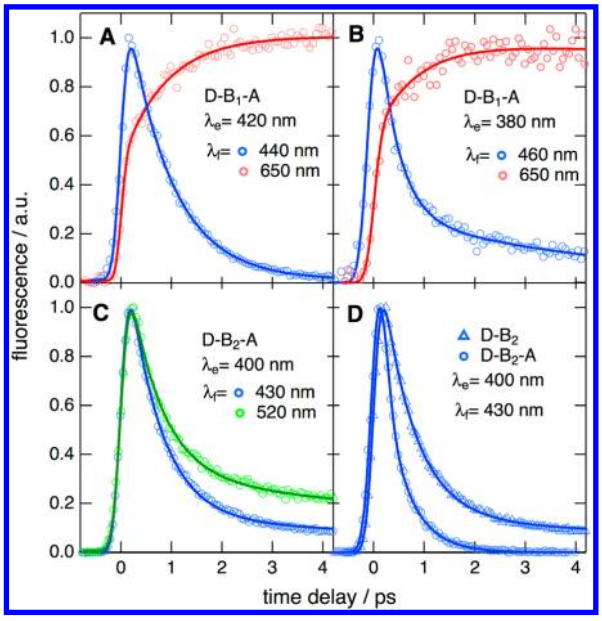

Figure 4. Time profiles of the fluorescence intensity measured by FU at different wavelengths (λ_f) upon excitation at various wavelengths (λ_e).

upon 420 nm (Soret band) excitation decays exponentially with a 820 fs time constant. At the same excitation wavelength, the time profile at 650 nm exhibits a prompt rise and a 800 fs rising component. The 800 fs time constant can be ascribed to the S_2−S_1 internal conversion in the ZnP unit, whereas the prompt rise is most probably due to fluorescence from FbP that is also directly excited at 420 nm. The shortening of the S_2 fluorescence lifetime from 1.5 ps in ZnP alone to 800 fs in D−B_1−A is most probably due to the perturbation of the electronic structure of ZnP introduced by the linkage to B_1. Such a decrease of the S_2 lifetime upon substitution of ZnP has already been reported earlier.[7,36,56,57]

The dynamics is more complex upon 380 nm excitation, where absorption from the bridge is important, although not exclusive. First, the decay of the emission at 460 nm is biphasic with 380 fs and 4 ps time constants, and with 0.8 and 0.2 relative amplitudes (Figure 4B). Second, the rise of the 650 nm emission still exhibits prompt and 800 fs rising components (Figure 4B). Given the absorption and emission spectra of B_1 (Figure 2), the emission at 460 nm should mostly originate from the bridge. Therefore, these 380 fs and 4 ps decay times should be compared to the 500 ps fluorescence lifetime of B_1 alone.[33] This huge acceleration when going from B_1 to D−B_1−A can be ascribed to a highly efficient EET from the bridge to the porphyrin ends, as already revealed by the stationary fluorescence spectrum upon 365 nm excitation. The reason for the biphasic nature of the decay of the bridge fluorescence is unclear but could be related to the distribution of torsion angles existing in the bridge itself and between the bridge and the porphyrins.[58−60]

According to the stationary fluorescence spectrum recorded upon bridge excitation, EET to the ZnP end is about twice as efficient as EET to the FbP end. Therefore, assuming an overall EET rate constant of $(0.38\ \text{ps})^{-1}$, one obtains bridge to ZnP and bridge to FbP EET rate constants of $(0.57\ \text{ps})^{-1}$ and $(1.14\ \text{ps})^{-1}$, respectively. In the case of ZnP, one can conclude from the 800 fs rise time of the 650 nm fluorescence upon bridge excitation that EET from the bridge results in the population of the local S_2 state of ZnP, which then undergoes internal conversion to the local S_1 state in 800 fs as also found upon direct Soret band excitation. The prompt rising component at 650 nm can be accounted for by direct excitation of FbP that also absorbs at 380 nm (Figure 2A).

Selective bridge or porphyrin excitation is not possible with D−B_2 and D−B_2−A, and all FU measurements were performed upon 400 nm excitation only. The fluorescence dynamics was measured at 430 and 520 nm. At 430 nm, emission mostly arises from the local S_2 ZnP state, whereas, at 520 nm, it should be mainly due to the bridge. For both D−B_2 and D−B_2−A, the fluorescence decays at these wavelengths are not exponential (Figure 4C,D) and need the sum of two or three exponential functions to be properly reproduced. In fact, the profiles measured with a given compound at 430 and 520 nm can be analyzed globally with the time constants listed in Table 1. The 850 ps time constant, which has a substantially larger amplitude at 520 nm than at 430 nm and is hardly visible with D−B_2−A, is identical to the lifetime of B_2 alone.[33] Therefore, we ascribe this 850 ps component to free B_2 impurities present in the D−B_2−A and D−B_2 samples. The relative amplitudes of the two other components at 430 and 520 nm are too similar to be explained in terms of the contribution of two different emitters, namely ZnP and bridge, especially considering that B_2 emits only weakly at 430 nm. The absorption spectra of D−B_2 and D−B_2−A show that the local S_2 ZnP state (D**−B_2−A) is almost isoenergetic with the local bridge S_1 state (D−B_2*−A) and with the local S_2 FbP state (D−B_2−A**). As a consequence, EET between these excited states should be reversible, except for that from D−B_2−A**, because of the ultrashort lifetime of this state, <50 fs for FbP alone.[61] In this case, the fluorescence dynamics in the 430−520 nm region can be discussed in terms of the scheme shown in Figure 5. This

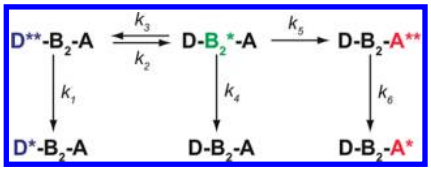

Figure 5. Kinetic scheme accounting for the fluorescence dynamics of D−B_2−A. The same can be used for D−B_2 with $k_5 = 0$.

scheme is essentially the same as that used for describing the fluorescence dynamics of excimers and exciplexes;[62,63] the only difference is the initial conditions as both the D**−B_2−A and D−B_2*−A states are directly populated upon optical excitation. Because of this, the solutions of the differential equations for D**−B_2−A and D−B_2*−A are much more complicated that those for the excimer/exciplex mechanism where only the excited precursor is initially populated, and are not only complex functions of all rate constants but also of the relative initial populations of D**−B_2−A and D−B_2*−A, which are not known. Because of the large number of adjustable parameters, a fit of these expressions to the experimental fluorescence time

dx.doi.org/10.1021/jp311540x | J. Phys. Chem. A 2013, 117, 918−928

profiles is pointless. Numerical simulations of ZnP and bridge fluorescence dynamics were first performed with D−B_2 assuming $k_1 = (1.4\ \text{ps})^{-1}$ and $k_4 = (850\ \text{ps})^{-1}$, i.e., the inverse fluorescence lifetimes of the individual constituents, and using different k_2 and k_3 values. This scheme yields biexponential kinetics, but the fast component appears as a rise in the time evolution of the ZnP or bridge fluorescence depending on whether k_2 is smaller or larger than k_3, respectively. On the other hand, if $k_2 = k_3$, only a minor rising component of the bridge fluorescence is predicted, but the decay is mono-exponential. Therefore, the observed fluorescence dynamics can only be satisfactorily reproduced if we assume that both ZnP and the bridge contribute to the emission at 520 nm and if k_2 and k_3 are between $(1\ \text{ps})^{-1}$ and $(0.3\ \text{ps})^{-1}$. Similar simulations show that the acceleration of the fluorescence decay observed by going from D−B_2 to D−B_2−A can be accounted for by the occurrence of EET from the bridge to the FbP end with a rate constant k_5 of the order of $(0.3–0.5\ \text{ps})^{-1}$. This transfer is irreversible because of the very large decay constant of the local S_2 FbP state, $k_6 = (0.05\ \text{ps})^{-1}$.

Such a scheme should of course not be considered too literally considering that the time scale on which the dynamics takes place is too short for an equilibrium to be established and that the electronic coupling between the chromophoric units should be relatively strong. In the strong coupling limit, excitation would be delocalized over both ZnP and bridge in D−B_2 and over all three chromophores in D−B_2−A.[64] In this case, the biphasic nature of the fluorescence decay could be explained by a distribution of geometries due to torsional disorder.[59,60]

Despite its crudeness, the scheme presented in Figure 5 and based on a localization of the excitation on either ZnP, the bridge, or FbP, gives a reasonable rationale of the observed fluorescence dynamics. Therefore, according to this model, stepwise EET from the ZnP end to the FbP end takes place on the subpicosecond time scale. According to the rate constants used for the simulation, the overall efficiency of this process should lie between 30 and 60%, assuming $k_1 = (1.4\ \text{ps})^{-1}$. However, this k_1 value of $(1.4\ \text{ps})^{-1}$ is probably underestimated considering the effect of substitution on the S_2 lifetime of ZnP observed with D−B_1−A. If $k_1 = (0.5\ \text{ps})^{-1}$, the overall EET efficiency falls to 20–40%.

Transient Absorption (TA) Spectroscopy. TA spectra recorded at different time delays after 400 nm excitation of D−B_1−A are illustrated in Figure 6A together with the negative stationary absorption spectrum. These spectra exhibit an intense negative band at 420 nm and a broad positive band culminating around 450 nm with a superimposed structure. This positive band can be ascribed to excited-state absorption, whereas the structure is due to the bleach of the ground-state population as well as the stimulated emission from the local S_1 ZnP and FbP states (Figure 2C).[64,65] Interestingly, the strong negative TA band at 420 nm is slightly blue shifted relative to the Soret band of D−B_1−A. This can be explained by the larger absorption coefficient of FbP at 400 nm compared to ZnP. Therefore, the Soret band of FbP that culminates at 419 nm is more bleached than that of ZnP, which peaks at 423 nm.

Only small changes in the TA spectra can be observed within the time window of the experiment that extends up to 2 ns. Global analysis of the TA spectra using a sum of exponential functions was performed to get a better insight into the origin of these changes.[66] The sum of four exponential functions was required to satisfactorily reproduce the time evolution of the

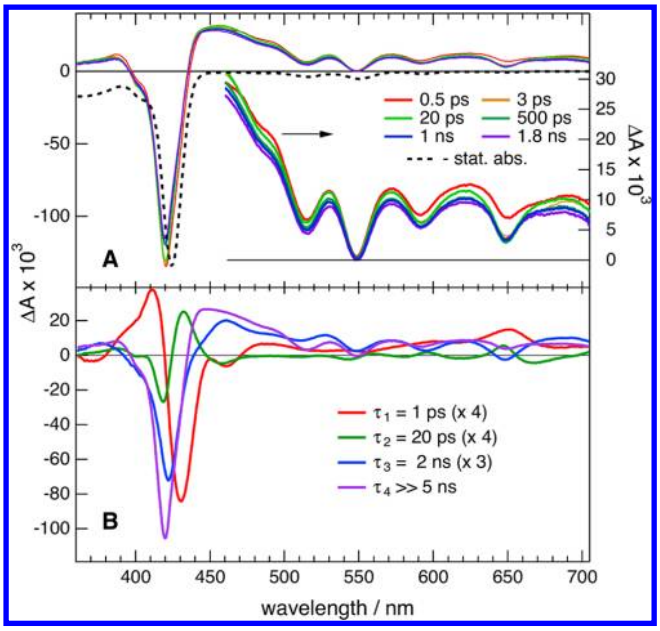

Figure 6. (A) TA spectra recorded at different time delays after 400 nm excitation of D−B_1−A and negative stationary absorption spectrum, and (B) decay-associated difference absorption spectra obtained upon global multiexponential analysis.

TA spectra; the decay-associated difference spectra (DADS) are depicted in Figure 6B. One of the time constants was fixed at 2 ns, the fluorescence lifetime of the ZnP unit, and the best fit values of the others were 1 ps, 20 ps, and ≫5 ns.

The spectrum associated with the ≫5 ns time constant contains the same features as those measured with ZnP and FbP, and can be ascribed to the local T_1 ZnP and S_1 FbP states.[65] The spectra associated with the other three decay times have all relatively small amplitude. The 1 ps component can be assigned to the decay of the local S_2 ZnP state. Indeed, the negative band at 430 nm in the DADS can be associated with the S_2–S_0 stimulated emission. Moreover, the positive band at 650 nm can be related to the population of the local S_1 ZnP state. These two features as well as the positive bands at 410 nm can also be observed with ZnP alone.[64] The 20 ps DADS has the smallest amplitude and is also similar to that observed with ZnP alone, associated with a 29 ps time constant and assigned to the vibrational relaxation of the S_1 state after ultrafast internal conversion.[64,67] We also interpret this time constant as the vibrational relaxation of both local S_1 ZnP and FbP states. The 2 ns time constant should reflect the decay of the local S_1 ZnP state population. However, the 2 ns DADS differs from that measured with ZnP alone, as it exhibits a negative band peaking at 423 nm, indicative of a recovery of the local ZnP ground state, whereas the DADS measured with ZnP alone does not exhibit this band.[64] Indeed, efficient intersystem crossing (ISC) in ZnP leaves the ground-state population depleted. This difference could be due to EET from the ZnP to the FbP end, taking place in parallel to ISC as found above with D−B_2−A. This process should lead to the recovery of the local ZnP ground state and to the depletion of that of FbP. The absence of a positive band at 419 nm reflecting an increase of FbP bleach could be explained by the somewhat smaller extinction coefficient of the Soret band of FbP compared to that of ZnP.

The bridge absorbs only weakly at 400 nm and is thus not expected to significantly contribute to the TA spectra.

dx.doi.org/10.1021/jp311540x | J. Phys. Chem. A 2013, 117, 918–928

Nevertheless, the 1 ps DADS shows a small negative feature around 370 nm that can be ascribed to the bleach of the bridge absorption band. Moreover, the bridge excited state has been shown to exhibit a broad absorption band above 500 nm,[33,43] and could be partially responsible for the broad positive band in the 1 ps spectrum. This result is consistent with the FU measurements that point to ultrafast EET from the bridge to both porphyrin ends. For D−B_1−A, EET only takes place from the bridge to the porphyrins, which, because of the lower energies of their excited states, act as energy traps.

TA spectra measured with D−B_2 upon 400 nm excitation are illustrated in Figure 7A. The main difference between these

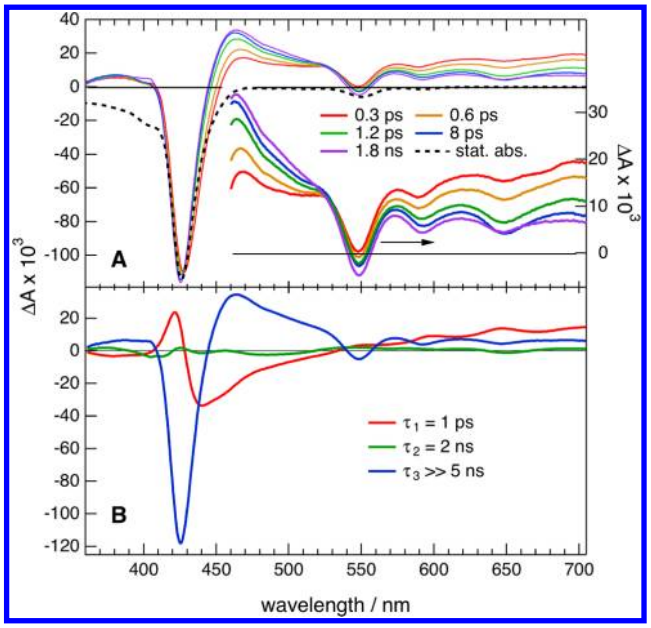

Figure 7. (A) TA spectra recorded at different time delays after 400 nm excitation of D−B_2 and negative stationary absorption spectrum, and (B) decay-associated difference absorption spectra obtained upon global multiexponential analysis.

spectra and those measured with D−B_1−A are (1) the exact coincidence of the negative TA band with the Soret band of D−B_2, in agreement with the fact that this band is due to ZnP only, (2) the absence of the 515 nm dip caused by the depletion of FbP ground-state population, and (3) substantially larger spectral changes taking place during the first 10 ps after excitation. Indeed, whereas the TA spectra recorded at the longest time delays are essentially the same as those measured with ZnP alone, the early TA spectra exhibit a weaker 450−500 nm band and a stronger band above 550 nm. The sum of three exponential functions was enough to reproduce the time evolution of these TA spectra, with 1 ps, ∼2 ns, and ≫5 ns time constants and with the DADS depicted in Figure 7B. The 1 ps DADS is similar to that found with D−B_1−A (Figure 6B), except for the negative band at 440 nm that has a much broader red wing. This latter feature can be ascribed to the stimulated emission from the bridge. This time constant can thus be assigned to the decay of the local S_2 ZnP state and of the local bridge excited state, in agreement with the FU measurements. The spectral changes taking place during the first picosecond are not large enough to resolve the two time constants found in the FU measurements. However, these TA results are consistent with either a fast equilibrium between D**−B_1−A and D−B_1*−A (Figure 5) or a delocalized excitation.

Given the time window of the TA experiment, the error on the 2 ns time constant is large and thus this value should be considered as approximate. This time constant can be ascribed to the decay of the local S_1 ZnP state by ISC. Contrary to the 2 ns DADS found with D−B_1−A, that of D−B_2 does not have a negative band at 423 nm and is very similar to that observed with ZnP alone. This strongly supports the above assumption that, in D−B_1−A, this component is partially due to EET from ZnP to FbP. As this process is not feasible in D−B_2, this 2 ns component is only due to ISC to the local T_1 ZnP state. Finally, the ≫5 ns DADS can be ascribed to the local T_1 ZnP state.

Finally, the TA spectra recorded with D−B_2−A (Figure 8A) contain features than can be recognized in those measured with

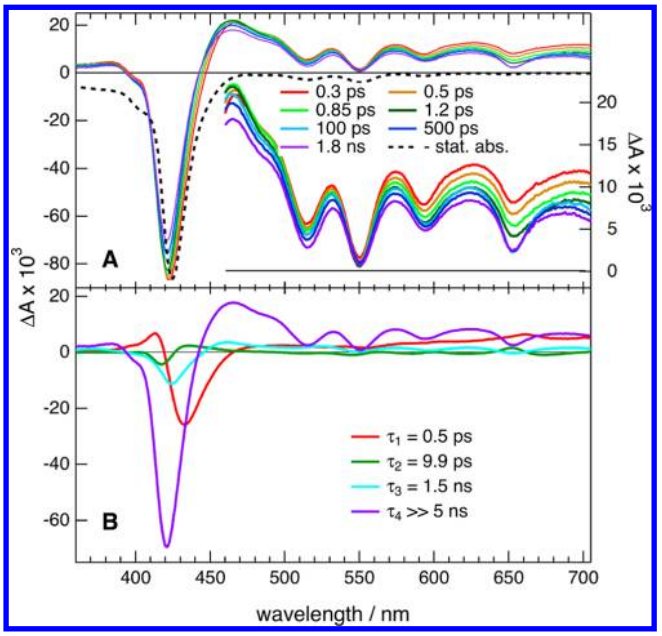

Figure 8. (A) TA spectra recorded at different time delays after 400 nm excitation of D−B_2−A and negative stationary absorption spectrum, and (B) decay-associated difference absorption spectra obtained upon global multiexponential analysis.

both D−B_1−A and D−B_2: (1) an intense negative band at 419 nm, blue shifted relative to the stationary absorption band of D−B_2−A, and a dip at 515 nm, due to the bleach of FbP, and (2) a substantial decrease of the signal above 550 nm during the first picosecond, due to the decay of the local bridge excited state. As for D−B_1−A, the sum of four exponential functions was required to reproduce the time evolution of the TA spectra with the time constants and DADS shown in Figure 8B. The 0.5 ps DADS contains features of both the local S_2 ZnP state and locally excited bridge, in good agreement with the FU results. Here again, the early changes in the TA spectra are too small to allow the two FU time constants to be resolved. The 10 ps DADS is very similar to the 20 ps DADS measured with D−B_1−A and is interpreted as well as the vibrational relaxation of both local S_1 ZnP and FbP states upon internal conversion. This difference of time constants is not really significant given the crudeness of the multiexponential analysis. Indeed, the early population dynamics takes place on the same time scale as vibrational relaxation,[68−70] and therefore, nonexponential dynamics can be expected. Consequently, the time constants obtained from an exponential analysis should only be considered as indications of the most relevant time scales.

dx.doi.org/10.1021/jp311540x | J. Phys. Chem. A 2013, 117, 918−928

Interestingly, the ~1.5 ns DADS differs from the ~2 ns found with D−B_2 but is very similar to that observed with D−B_1−A, and ascribed to the parallel occurrence of ISC in the ZnP moiety and EET from the ZnP to the FbP end. This interpretation is reinforced here as EET has indeed been evidenced by the shortening of the local S_1 ZnP fluorescence by going from D−B_2 to D−B_2−A. Finally, the ≫5 ns DADS is also very similar to that found with D−B_1−A and can be ascribed to the long-lived excited-state populations.

DISCUSSION

The rate constants of the various processes occurring upon photoexcitation of the D−B−A's are summarized in Figure 9.

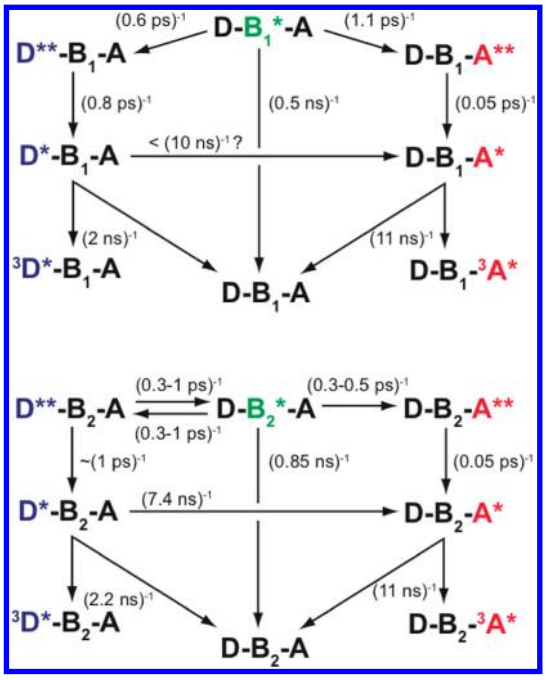

Figure 9. Summary of the conversion processes between the electronic states of the D−B−A's.

Various EETs are taking place on vastly different time scales. In principle, both Coulombic and exchange interactions could be responsible for EET; i.e., both Förster and Dexter EET can be operative. Therefore, in the weak coupling limit, the EET rate constant can be expressed as[71,72]

$$k_{EET} = \frac{2\pi}{\hbar}V^2\Theta \approx \frac{2\pi}{\hbar}(V_c^2 + V_e^2)\Theta \quad (1)$$

where V_c and V_e are the coupling energies associated with the Coulombic and exchange interactions, respectively, and Θ is the spectral overlap integral, calculated by taking the area normalized emission and absorption spectra of the energy donor and acceptor, respectively.

By comparing the lifetimes of the ZnP localized S_1 fluorescence of D−B_2−A and D−B_2, one can conclude that the rate constant of S_1 energy transfer from ZnP to FbP should amount to $(7.4\ ns)^{-1}$. According to eq 1 and to the Θ value calculated for this donor/acceptor pair (Table S1, Supporting Information), such an EET rate constant requires a coupling energy of 1.4 cm^{-1}. The origin of this coupling can be determined by comparing this value with that of V_c calculated within the point dipole approximation:[73,74]

$$V_c = \frac{f_L^{\,2}\mu_D\mu_A\kappa}{4\pi\varepsilon_0\varepsilon_{op}d^3} \quad (2)$$

where $f_L = (\varepsilon_{op} + 2)/3$ is the Lorentz correction factor; $\varepsilon_{op} \approx n^2$ is the dielectric constant at optical frequencies and is approximately equal to the square of the refractive index; n, μ_D, and μ_A are the magnitudes of the transition dipole moments for emission of the donor and absorption of the acceptor; κ is the orientation factor, which depends on the angles β_D and β_A between the dipoles and the center-to-center distance vector, $\vec{d}$, between donor and acceptor, respectively, and on the angle ϕ between the porphyrin planes. According to quantum chemical calculations, the center-to-center distance $d = |\vec{d}|$ amounts to 4.75 nm, whereas ϕ is equal to 47°. However, the barrier for torsion of the porphyrins around the bond with the bridge is low,[58] and thus a distribution of the angle ϕ should be assumed.

The calculation of V_c is further complicated by the degeneracy of the Q_x and Q_y transitions in ZnP and of their quasi-degeneracy in FbP.[75] Therefore, V_c can be seen as resulting from the interaction of two pairs of perpendicular transition dipoles. By taking a value of 2.25 D for each of these dipoles,[7] and assuming an angle ϕ evenly distributed between 0 and 180°, a V_c value of 0.56 cm^{-1} is obtained (see Supporting Information). The difference between this value and that of 1.4 cm^{-1} obtained from the EET rate constant is most probably due to the exchange interaction mediated by the bridge.[76] This effect has been investigated in detail by Albinsson and co-workers, who showed that the exponential decrease of V_e with increasing donor−acceptor distance depends on the energy gap between the bridge and donor excited states.[24,26,30,77] As this gap is smaller for B_2 than for B_1, this bridge-mediated EET can be expected to be more important in D−B_2−A than in D−B_1−A. Unfortunately, for the latter system, no reliable EET rate constant can be deduced from the TA data.

The same approach has been tentatively used for the EET processes involving the bridge. In D−B_1−A, bridge to porphyrin EET can be clearly seen from stationary and time-resolved fluorescence. From eq 1 and the spectral overlap integral listed in Table S1 (See Supporting Information), the coupling energies for EET from B_1 to ZnP and from B_1 to FbP with time constants of 0.57 and 1.14 ps, respectively, amount to 64 and 48 cm^{-1}. The local S_1−S_0 transition dipole moment of the bridge amounts to 13.4 D,[33] whereas those responsible for the Soret band of the porphyrins are doubly degenerate with a value of about 7.8 D each.[7] Using eq 2 with a d value of 2.36 nm results in V_c= 72 cm^{-1} (see Supporting Information), a value that exceeds that deduced from the EET rate constant. This outcome is probably a consequence of the failure of the point dipole approximation when the transition dipole moments are very large and the distance between the chromophoric units is small.[78] Furthermore, eq 1 is only valid in the weak coupling limit. This is the case for the S_1 EET from ZnP to FbP, as testified to by the absorption spectra of the D−B−A's in the Q-band region that are the composite of those of the individual chromophores. This is however no longer the case in the Soret band region, where substantial shift and broadening can be observed. Moreover, the exchange interaction can be expected to be operative as well. In any case, these simple considerations shows that bridge to porphyrin EET on the subpicosecond time scale is not unrealistic.

dx.doi.org/10.1021/jp311540x | J. Phys. Chem. A 2013, 117, 918−928

EET to and from the bridge in D−B_2−A seems to occur on a time scale similar to that in D−B_1−A. The use of eq 1 to discuss these processes is certainly even less adequate than for D−B_1−A. Indeed, the bridge and porphyrin states are quasi degenerate, and because of this, the electronic excitation is probably not fully localized. This is also supported by the quantum chemistry calculations that reveal the existence of several MOs where the density spills out of the porphyrin to the bridge. On the other hand, the coupling is not strong enough to result in excitonic states where the excitation is fully delocalized on the whole molecule. If this were the case, the absorption spectrum of D−B_2−A in the Soret band region would differ much more from those of the constituents.[74]

CONCLUDING REMARKS

We have investigated D−B−A systems consisting of two porphyrins separated by more than 4.5 nm using bridges with the lowest excited state close to the S_2 porphyrin states. This bridge produces only little perturbation on the local S_1 porphyrin states, and therefore S_1 energy transfer from ZnP to FbP is observed on the nanosecond time scale. However, substantial coupling between the bridge and upper porphyrin states takes place. When the bridge state is higher than the S_2 porphyrin states, as is the case with the oligophenyleneethynylene bridge, ultrafast energy transfer from the bridge to the porphyrin ends is observed. This process results in the population of the porphyrins' S_2 states and is followed by internal conversion to their S_1 states. Thus no S_2 energy transfer from the porphyrin to the bridge is observed in this case. The presence of alkoxy substituents on the bridge lowers its excited-state energy to a value very close to those of the porphyrin S_2 states so that conversion between these states by energy transfer on the 1 ps time scale becomes operative. As a consequence, a net S_2 energy transfer with an efficiency of 0.2−0.6 takes place from the ZnP to the FbP end, located at about 4.7 nm, within a picosecond. Unfortunately, Soret band excitation of the ZnP end cannot be done selectively, and therefore, this ultrafast translocation of energy over a long distance is partially hidden by the dynamics associated with the direct excitation of the other units. For this approach to be really useful, one would have to further lower the energy of the bridge excited state to avoid direct excitation and reversible energy transfer. Finally, FbP should be replaced by a chromophore with the S_1 energy just below the bridge excited state, for example, a boron−dipyrromethene dye.

ASSOCIATED CONTENT

Supporting Information

Frontier molecular orbitals of the D−B−A's, fluorescence excitation spectra of D−B_1−A, analysis of the fluorescence spectrum of D−B_1−A upon bridge excitation, fluorescence spectrum of D−B_2−A in the 400−550 nm region, TCSPC fluorescence decays measured with D−B_1−A, calculation of V_c, and spectral overlap integrals Θ. This material is available free of charge via the Internet at http://pubs.acs.org.

AUTHOR INFORMATION

Corresponding Author

*E-mail: eric.vauthey@unige.ch.

Notes

The authors declare no competing financial interest.

ACKNOWLEDGMENTS

The authors wish to thank Prof. A. Gossauer (Department of Chemistry, University of Fribourg) for the compounds and the Fonds National Suisse de la Recherche Scientifique (Project No. 200020-124393) as well as the University of Geneva for financial support.

REFERENCES

(1) Davila, J.; Harriman, A.; Milgrom, L. R. A Light Harvesting Array of Synthetic Porphyrins. *Chem. Phys. Lett.* **1987**, *136*, 427−430.

(2) Gust, D.; Moore, T. A.; Moore, A. L.; Gao, F.; Luttrull, D.; DeGraziano, J. M.; Ma, X. C.; Makings, L. R.; Lee, S.-J.; Trier, T. T.; et al. Long-Lived Photoinitiated Charge Separation in Carotene Diporphyrin Triad Molecules. *J. Am. Chem. Soc.* **1991**, *113*, 3638−3649.

(3) Li, F.; Yang, S. I.; Ciringh, Y.; Seth, J.; Martin, C. H., III; Singh, D. L.; Kim, D.; Birge, R. R.; Bocian, D. F.; Holten, D.; Lindsey, J. S. Design, Synthesis and Photodynamics of Light Harvesting Arrays Comprised of a Porphyrin and One, Two or Eight Boron-Dipyrrin Accessory Pigments. *J. Am. Chem. Soc.* **1998**, *120*, 10001−10017.

(4) Brodard, P.; Matzinger, S.; Vauthey, E.; Mongin, O.; Papamicaël, C.; Gossauer, A. Investigations of Electronic Energy Transfer Dynamics in Multiporphyrin Arrays. *J. Phys. Chem. A* **1999**, *103*, 5858−5870.

(5) Yeow, E. K. L.; Ghiggino, K. P.; Reek, J. N. H.; Crossley, M. J.; Bosman, A. W.; Schenning, A. P. H. J.; Meijer, E. W. The Dynamics of Electronic Energy Transfer in Novel Multiporphyrin Functionalized Dendrimers: A Time-Resolved Fluorescence Anisotropy Study. *J. Phys. Chem. B* **2000**, *104*, 2596−2606.

(6) Holten, D.; Bocian, D. F.; Lindsey, J. S. Probing Electronic Communication in Covalently Linked Multiporphyrin Arrays. A Guide to the Rational Design of Molecular Photonics Devices. *Acc. Chem. Res.* **2002**, *35*, 57.

(7) Morandeira, A.; Vauthey, E.; Schuwey, A.; Gossauer, A. Ultrafast Excited State Dynamics of Tri- and Hexaporphyrin Arrays. *J. Phys. Chem. A* **2004**, *108*, 5741−5751.

(8) Borgström, M.; Shaikh, N.; Johansson, O.; Anderlund, M. F.; Styring, S.; Aakermark, B.; Magnuson, A.; Hammarström, L. Light Induced Manganese Oxidation and Long-Lived Charge Separation in a $Mn_2^{II,II}$-$Ru^{II}(bpy)_3$-Acceptor Triad. *J. Am. Chem. Soc.* **2005**, *127*, 17504−17515.

(9) Wasielewski, M. R. Energy, Charge, and Spin Transport in Molecules and Self-Assembled Nanostructures Inspired by Photosynthesis. *J. Org. Chem.* **2006**, *71*, 5051−5066.

(10) Kodis, G.; Terazono, Y.; Liddell, P. A.; Andréasson, J.; Garg, V.; Hambourger, M.; Moore, T. A.; Moore, A. L.; Gust, D. Energy and Photoinduced Electron Transfer in a Wheel-Shaped Artificial Photosynthetic Antenna-Reaction Center Complex. *J. Am. Chem. Soc.* **2006**, *128*, 1818.

(11) Bhosale, S.; Sisson, A. L.; Talukdar, P.; Fürstenberg, A.; Banerji, N.; Vauthey, E.; Bollot, G.; Mareda, J.; Röger, C.; Würthner, F.; et al. Photoproduction of Proton Gradients with π-Stacked Fluorophore Scaffolds in Lipid Bilayers. *Science* **2006**, *313*, 84−86.

(12) Kelley, R. F.; Goldsmith, R. H.; Wasielewski, M. R. Ultrafast Energy Transfer within Cyclic Self-Assembled Chlorophyll Tetramers. *J. Am. Chem. Soc.* **2007**, *129*, 6384−6385.

(13) Mongin, O.; Pla-Quintana, A.; Terenziani, F.; Drouin, D.; Le Droumaget, C.; Caminade, A.-M.; Majoral, J.-P.; Blanchard-Desce, M. Organic Nanodots for Multiphotonics: Synthesis and Photophysical Studies. *New J. Chem.* **2007**, *31*, 1354−1367.

(14) Gust, D.; Moore, T. A.; Moore, A. L. Solar Fuels via Artificial Photosynthesis. *Acc. Chem. Res.* **2009**, *42*, 1890−1898.

(15) Aratani, N.; Kim, D.; Osuka, A. Discrete Cyclic Porphyrin Arrays as Artificial Light-Harvesting Antenna. *Acc. Chem. Res.* **2009**, *42*, 1922−1934.

(16) O'Sullivan, M. C.; Sprafke, J. K.; Kondratuk, D. V.; Rinfray, C.; Claridge, T. D. W.; Saywell, A.; Blunt, M. O.; O'Shea, J. N.; Beton, P.

H.; Malfois, M.; et al. Vernier Templating and Synthesis of a 12-Porphyrin Nano-Ring. *Nature* **2011**, *469*, 72−75.
(17) Sakai, N.; Lista, M.; Kel, O.; Sakurai, S.-i.; Emery, D.; Mareda, J.; Vauthey, E.; Matile, S. Self-Organizing Surface-Initiated Polymerization: Facile Access to Complex Functional Systems. *J. Am. Chem. Soc.* **2011**, *133*, 15224−15227.
(18) Grimm, B.; Schornbaum, J.; Jasch, H.; Trukhina, O.; Wessendorf, F.; Hirsch, A.; Torres, T.; Guldi, D. M. Step-by-Step Self-Assembled Hybrids that Feature Control over Energy and Charge Transfer. *Proc. Natl. Acad. Sci. U.S.A.* **2012**, *109*, 15565−15571.
(19) Oevering, H.; Paddon-Row, M. N.; Heppener, M.; Oliver, A. M.; Cotsaris, E.; Verhoeven, J. W.; Hush, N. S. Long-Range Photoinduced Through-Bond Electron Transfer and Radiative Recombination via Rigid Non-Conjugated Bridges: Distance and Solvent Dependence. *J. Am. Chem. Soc.* **1987**, *109*, 3258−3269.
(20) Closs, G. L.; Johnson, M. D.; Miller, J. R.; Piotrowiak, P. A Connection between Intramolecular Long-Range Electron, Hole and Triplet Energy Transfer. *J. Am. Chem. Soc.* **1989**, *111*, 3751−3753.
(21) Ratner, M. A. Bridge Assisted Electron Transfer: Effective Electronic Coupling. *J. Phys. Chem.* **1990**, *94*, 4877−4883.
(22) Kroon, J.; Oliver, A. M.; Paddon-Row, M. N.; Verhoeven, J. W. Observation of a Remarkable Dependence of the Rate of Singlet-Singlet Energy Transfer on the Configuration of the Hydrocarbon Bridge in Bichromophoric Systems. *J. Am. Chem. Soc.* **1990**, *112*, 4868−4873.
(23) Scholes, G. D.; Ghiggino, K. P.; Oliver, A. M.; Paddon-Row, M. N. Intramolecular Electronic Energy Transfer between Rigidly Linked Naphthalene and Anthracene Chromophores. *J. Phys. Chem.* **1993**, *97*, 11871−11876.
(24) Kilså, K.; Kajanus, J.; Mårtensson, J.; Albinsson, B. Mediated Electronic Coupling: Singlet Energy Transfer in Porphyrin Dimers Enhanced by the Bridging Chromophore. *J. Phys. Chem. B* **1999**, *103*, 7329−7339.
(25) Piet, J. J.; Taylor, P. N.; Wegewijs, B. R.; Anderson, H. L.; Osuka, A.; Warman, J. M. Photoexcitations of Covalently Bridged Zinc Porphyrin Oligomers: Frenkel versus Wannier-Mott Type Excitons. *J. Phys. Chem. B* **2001**, *105*, 97−104.
(26) Albinsson, B.; Mårtensson, J. Long-Range Electron and Excitation Energy Transfer in Donor-Bridge-Acceptor Systems. *J. Photochem. Photobiol., C* **2008**, *9*, 138−155.
(27) Chaignon, F.; Falkenstrom, M.; Karlsson, S.; Blart, E.; Odobel, F.; Hammarström, L. Very Large Acceleration of the Photoinduced Electron Transfer in a Ru(bpy)3-Naphthalene Bisimide Dyad Bridged on the Naphthyl Core. *Chem. Commun.* **2007**, 64−66.
(28) Wiberg, J.; Guo, L.; Petterson, K.; Nilsson, D.; Ljungdahl, T.; Mårtensson, J.; Albinsson, B. Charge Recombination versus Charge Separation in Donor-Bridge-Acceptor Systems. *J. Am. Chem. Soc.* **2007**, *129*, 155−163.
(29) Wenger, O. S. How Donor-Bridge-Acceptor Energetics Influence Electron Tunneling Dynamics and Their Distance Dependences. *Acc. Chem. Res.* **2011**, *44*, 25−35.
(30) Winters, M. U.; Pettersson, K.; Martensson, J.; Albinsson, B. Competition between Superexchange Mediated and Sequential Electron Transfer in a Bridged Donor-Acceptor System. *Chem.—Eur. J.* **2005**, *11*, 562−573.
(31) Weiss, E. A.; Tauber, M. J.; Kelley, R. F.; Ahrens, M. J.; Ratner, M. A.; Wasielewski, M. R. Conformationally Gated Switching between Superexchange and Hopping within Oligo-p-phenylene-Based Molecular Wires. *J. Am. Chem. Soc.* **2005**, *127*, 11842−11850.
(32) Paulson, B. P.; Miller, J. R.; Gan, W.-X.; Closs, G. Superexchange and Sequential Mechanisms in Charge Transfer with a Mediating State between the Donor and Acceptor. *J. Am. Chem. Soc.* **2005**, *127*, 4860−4868.
(33) Duvanel, G.; Grilj, J.; Schuwey, A.; Gossauer, A.; Vauthey, E. Ultrafast Excited-State Dynamics of Phenyleneethynylene Oligomers in Solution. *Photochem. Photobiol. Sci.* **2007**, *6*, 956−963.
(34) Gurzadyan, G. G.; Tran-Thi, T.-H.; Gustavsson, T. Time-Resolved Fluorescence Spectroscopy of High-Lying Electronic States of Zn-Tetraphenylporphyrin. *J. Chem. Phys.* **1998**, *108*, 385−388.
(35) Liu, H. Z.; Baskin, J. S.; Steiger, B.; Wan, C. Z.; Anson, F. C.; Zewail, A. H. Femtosecond Dynamics of Metalloporphyrins: Electron Transfer and Energy Redistribution. *Chem. Phys. Lett.* **1998**, *293*, 1−8.
(36) Liu, X.; Tripathy, U.; Bhosale, S. V.; Langford, S. J.; Steer, R. P. Photophysics of Soret-Excited Tetrapyrroles in Solution. II. Effects of Perdeuteration, Substituent Nature and Position, and Macrocycle Structure and Conformation in Zinc(II) Porphyrins. *J. Phys. Chem. A* **2008**, *112*, 8986−8998.
(37) Nakano, A.; Yasuda, Y.; Yamasaki, T.; Akimoto, S.; Yamazaki, I.; Miyasaka, H.; Itaya, A.; Murakami, M.; Osuka, A. Intramolecular Energy Transfer in S_1- and S_2-States of Porphyrin Trimers. *J. Phys. Chem. A* **2001**, *105*, 4822−4833.
(38) Muller, P.-A.; Högemann, C.; Allonas, X.; Jacques, P.; Vauthey, E. Deuterium Isotope Effect on the Charge Recombination Dynamics of Contact Ion Pairs Formed by Electron Transfer Quenching in Acetonitrile. *Chem. Phys. Lett.* **2000**, *326*, 321−327.
(39) Morandeira, A.; Fürstenberg, A.; Gumy, J.-C.; Vauthey, E. Fluorescence Quenching in Electron Donating Solvents. 1. Influence of the Solute-Solvent Interactions on the Dynamics. *J. Phys. Chem. A* **2003**, *107*, 5375−5383.
(40) Morandeira, A.; Engeli, L.; Vauthey, E. Ultrafast Charge Recombination of Photogenerated Ion Pairs to an Electronic Excited State. *J. Phys. Chem. A* **2002**, *106*, 4833−4837.
(41) Duvanel, G.; Grilj, J.; Chaumeil, H.; Jacques, P.; Vauthey, E. Ultrafast Excited-State Dynamics of a Series of Zwitterionic Pyridinium Phenoxides with Increasing Sterical Hindering. *Photochem. Photobiol. Sci.* **2010**, *9*, 908−915.
(42) Duvanel, G.; Banerji, N.; Vauthey, E. Excited-State Dynamics of Donor-Acceptor Bridged Systems Containing a Boron-Dipyrromethene Chromophore: Interplay between Charge Separation and Reorientational Motion. *J. Phys. Chem. A* **2007**, *111*, 5361−5369.
(43) Banerji, N.; Duvanel, G.; Perez-Velasco, A.; Maity, S.; Sakai, N.; Matile, S.; Vauthey, E. Excited-State Dynamics of Hybrid Multichromophoric Systems: Toward an Excitation Wavelength Control of the Charge Separation Pathways. *J. Phys. Chem. A* **2009**, *113*, 8202−8212.
(44) Perdew, J. P. Density-Functional Approximation for the Correlation Energy of the Inhomogeneous Electron Gas. *Phys. Rev. B* **1986**, *33*, 8822−8824.
(45) Schäfer, A.; Horn, H.; Ahlrichs, R. Fully Optimized Contracted Gaussian Basis Sets for Atoms Li to K. *J. Chem. Phys.* **1992**, *97*, 2571−2577.
(46) Bauernschmitt, R.; Ahlrichs, R. Treatment of Electronic Excitations within the Adiabatic Approximation of Time Dependent Density Functional Theory. *Chem. Phys. Lett.* **1996**, *256*, 454−464.
(47) Ahlrichs, R.; Bär, M.; Häser, M. Electronic Structure Calculations on Workstation Computers: The Program System Turbomole. *Chem. Phys. Lett.* **1989**, *162*, 165−169.
(48) Gouterman, M. Spectra of Porphyrins. *J. Mol. Spectrosc.* **1961**, *6*, 138−163.
(49) Magyar, R. J.; Tretiak, S.; Gao, Y.; Wang, H.-L.; Shreve, A. P. A Joint Theoretical and Experimental Study of Phenylene−Acetylene Molecular Wires. *Chem. Phys. Lett.* **2005**, *401*, 149−156.
(50) Sluch, M. I.; Godt, A.; Bunz, U. H. F.; Berg, M. A. Excited-State Dynamics of Oligo(p-phenyleneethynylene): Quadratic Coupling and Torsional Motions. *J. Am. Chem. Soc.* **2001**, *123*, 6447−6448.
(51) Liu, L. T.; Yaron, D. J.; Sluch, M. I.; Berg, M. A. Modelling the Effect of Torsional Disorder on the Spectra of Poly- and Oligo-(*p*-phenyleneethylenes). *J. Phys. Chem. B* **2006**, *110*, 18844−18852.
(52) Dreuw, A.; Head-Gordon, M. Failure of Time-Dependent Density Functional Theory for Long-Range Charge-Transfer Excited States: The Zincbacteriochlorin−Bacteriochlorin and Bacteriochlorophyll−Spheroidene Complexes. *J. Am. Chem. Soc.* **2004**, *126*, 4007−4016.
(53) Karolczak, J.; Kowalska, D.; Lukaszewicz, A.; Maciejewski, A.; Steer, R. P. Photophysical Studies of Porphyrins and Metalloporphyrins: Accurate Measurements of Fluorescence Spectra and Fluorescence Quantum Yields for Soret Band Excitation of Zinc Tetraphenylporphyrin. *J. Phys. Chem. A* **2004**, *108*, 4570−4575.

(54) Ohno, O.; Kaizu, Y.; Kobayashi, H. Luminescence of some Metalloporphins Including the Complexes of the IIIb Metal Group. *J. Chem. Phys.* **1985**, *82*, 1779−1787.
(55) Quimby, D. J.; Longo, F. R. Luminescence Studies on several Tetraarylporphins and their Zinc Derivatives. *J. Am. Chem. Soc.* **1975**, *97*, 5111−5117.
(56) Cho, H. S.; Song, N. W.; Kim, Y. H.; Jeoung, S. C.; Hahn, S.; Kim, D.; Kim, S. K.; Yoshida, N.; Osuka, A. Ultrafast Energy Relaxation Dynamics of Directly Linked Porphyrin Arrays. *J. Phys. Chem. A* **2000**, *104*, 3287−3298.
(57) Villamaina, D.; Bhosale, S.; Langford, S. J.; Vauthey, E. Excited-State Dynamics of Porphyrin-Naphthalenediimide-Porphyrin Triads. *Phys. Chem. Chem. Phys.* **2013**, *15*, 1177−1187.
(58) Petterson, K.; Kyrychenko, A.; Rönnow, E.; Ljungdahl, T.; Mårtensson, J.; Albinsson, B. Singlet Energy Transfer in Porphyrin-Based Donor-Bridge-Acceptor Systems: Interaction between Bridge Length and Bridge Energy. *J. Phys. Chem. A* **2006**, *110*, 310−318.
(59) Edholm, O.; Blomberg, C. Stretched Exponentials and Barrier Distributions. *Chem. Phys.* **1999**, *252*, 221−225.
(60) Wlodarczyk, J.; Kierdaszuk, B. Interpretation of Fluorescence Decays Using a Power-like Model. *Biophys. J.* **2003**, *85*, 589−598.
(61) Baskin, J. S.; Yu, H.-Z.; Zewail, A. H. Ultrafast Dynamics of Porphyrins in the Condensed Phase: I. Free Base Tetraphenylporphyrin. *J. Phys. Chem. A* **2002**, *106*, 9837−9844.
(62) Birks, J. B. *Photophysics of Aromatic Molecules*; Wiley: New York, 1970.
(63) Hui, M.-H.; Ware, W. R.; Exciplex Photophysics, V. The Kinetics of Fluorescence Quenchin of Anthracene by *N*,*N*-Dimethylaniline in Cyclohexane. *J. Am. Chem. Soc.* **1976**, *98*, 4718−4727.
(64) Banerji, N.; Bhosale, S. V.; Petkova, I.; Langford, S. J.; Vauthey, E. Ultrafast Excited-State Dynamics of Strongly Coupled Porphyrin/Core-Substituted-Naphthalenediimide Dyads. *Phys. Chem. Chem. Phys.* **2011**, *13*, 1019−1029.
(65) Rodriguez, J.; Kirmaier, C.; Holten, D. Optical Properties of Metalloporphyrin Excited States. *J. Am. Chem. Soc.* **1989**, *111*, 6500−6506.
(66) van Stokkum, I. H. M.; Larsen, D. S.; van Grondelle, R. Global and Target Analysis of Time-Resolved Spectra. *Biochim. Biophys. Acta, Bioenerg.* **2004**, *1657*, 82−104.
(67) Yu, H.-Z.; Baskin, J. S.; Zewail, A. H. Ultrafast Dynamics of Porphyrins in the Condensed Phase: II. Zinc Tetraphenylporphyrin. *J. Phys. Chem. A* **2002**, *106*, 9845−9854.
(68) Elsaesser, T.; Kaiser, W. Vibrational and Vibronic Relaxation of Large Polyatomic Molecules in Liquids. *Annu. Rev. Phys. Chem.* **1991**, *42*, 83−107.
(69) Kovalenko, S. A.; Schanz, R.; Hennig, H.; Ernsting, N. P. Cooling Dynamics of an Optically Excited Molecular Probe in Solution from Femtosecond Broadband Transient Absorption Spectroscopy. *J. Chem. Phys.* **2001**, *115*, 3256−3274.
(70) Pigliucci, A.; Duvanel, G.; Lawson Daku, M. L.; Vauthey, E. Investigation of the Influence of Solute-Solvent Interactions on the Vibrational Energy Relaxation Dynamics of Large Molecules in Liquids. *J. Phys. Chem. A* **2007**, *111*, 6135−6145.
(71) Förster, T. Energy Migration and Fluorescence. *Naturwissenschaften* **1946**, *33*, 166−175.
(72) Dexter, D. L. A Theory of Sensitized Luminescence in Solids. *J. Chem. Phys.* **1953**, *21*, 836−850.
(73) Pullerits, T.; Hess, S.; Herek, J. L.; Sundström, V. Temperature Dependence of Excitation Transfer in LH2 of Rhodobacter Sphaeroides. *J. Phys. Chem. B* **1997**, *101*, 10560−10567.
(74) van Amerongen, H.; Valkunas, L.; van Grondelle, R. *Photosynthetic Excitons*; World Scientific: Singapore, 2000.
(75) Mårtensson, J. Calculation of the Förster Orientation Factor for Donor-Acceptor Systems with One Chromophore of Threefold or Higher Symmetry: Zinc Porphyrin. *Chem. Phys. Lett.* **1994**, *229*, 449−456.
(76) Hsiao, J. S.; Krueger, B. P.; Wagner, R. W.; Johnson, T. E.; Delaney, J. K.; Mauzerall, D. C.; Fleming, G. R.; Lindsey, J. S.; Bocian, D. F.; Donohoe, R. J. Soluble Synthetic Multiporphyrin Arrays. 2. Photodynamics of Energy Transfer Processes. *J. Am. Chem. Soc.* **1996**, *118*, 11181−11193.
(77) Pettersson, K.; Wiberg, J.; Ljungdahl, T.; Mårtensson, J.; Albinsson, B. Interplay between Barrier Width and Height in Electron Tunneling: Photoinduced Electron Transfer in Porphyrin-Based Donor-Bridge-Acceptor Systems. *J. Phys. Chem. A* **2006**, *110*, 319−326.
(78) Scholes, G. D.; Jordanides, X. J.; Fleming, G. R. Adapting the Förster Theory of Energy Transfer for Modeling Dynamics in Aggregated Molecular Assemblies. *J. Phys. Chem. B* **2001**, *105*, 1640−1651.